

PDF4LHC benchmark results from NNPDF

The NNPDF Collaboration:

Richard D. Ball¹, Luigi Del Debbio¹, Stefano Forte²,
Alberto Guffanti³, José I. Latorre⁴, Juan Rojo² and Maria Ubiali^{1,5}.

¹ *School of Physics and Astronomy, University of Edinburgh,
JCMB, KB, Mayfield Rd, Edinburgh EH9 3JZ, Scotland*

² *Dipartimento di Fisica, Università di Milano and INFN, Sezione di Milano,
Via Celoria 16, I-20133 Milano, Italy*

³ *Physikalisches Institut, Albert-Ludwigs-Universität Freiburg
Hermann-Herder-Straße 3, D-79104 Freiburg i. B., Germany*

⁴ *Departament d'Estructura i Constituents de la Matèria, Universitat de Barcelona,
Diagonal 647, E-08028 Barcelona, Spain*

⁵ *Center for Particle Physics Phenomenology CP3, Université Catholique de Louvain,
Chemin du Cyclotron, 1348 Louvain-la-Neuve, Belgium*

Abstract:

We present the results for the PDF4LHC benchmark processes obtained with the NNPDF2.0 set. Our results include the combination of PDF and α_s uncertainties, the comparison of 1-sigma and 68% C.L. uncertainties as well as the determination on the uncertainties on the PDF uncertainties themselves.

1 PDF4LHC Benchmark settings

The present study is based on the NNPDF2.0 parton set [1]. The NNPDF2.0 reference set uses $\alpha_s(M_Z^2) = 0.119$, fits with different value of α_s , in the range $0.114 \leq \alpha_s \leq 0.124$, are also discussed in [1] and can be obtained from the NNPDF website,

<http://sophia.ecm.ub.es/nnpdf>

In the rest of this note we will take as reference value for α_s and its uncertainty the following range:

$$\alpha_s(M_Z^2) = 0.119 \pm 0.002 \text{ (68\% C.L.)} , \quad (1)$$

The list of benchmark processes which we have considered, both at LHC 14 TeV and at LHC 7 TeV, are

- W^+ and W^- production
- Z^0 production
- H production through gg fusion at $m_H = 120, 180$ and 240 GeV
- $t\bar{t}$ production for $m_t = 171.3$ GeV.

These benchmark processes have been computed using a dedicated version of the MCFM code. On top of these, we have also produced benchmark results for the inclusive jet production at the Tevatron, using the FastNLO.

For the total cross sections, we provide both tables with the benchmark results as well as a graphical representation of these. We will provide results for both 1- σ errors and 68% Confidence Level errors. We provide the results for all processes and its associated uncertainties obtained from PDF sets with different values of α_s , as well as the combined PDF+ α_s uncertainty assuming Eq. 1.

2 Combination of PDF and α_s uncertainties

The methodology used within the NNPDF approach to combine PDF and α_s uncertainties was discussed in Refs. [2,3]. In particular, in Ref. [?] the NNPDF prescription to combine PDF and α_s uncertainties was compared to the corresponding prescriptions from MSTW and CTEQ in the case of Higgs production through gluon-gluon fusion. This methodology is briefly reviewed here.

The simplest approach consist in adding in quadrature the PDF and α_s uncertainties. using PDFs obtained from different values of α_s : this way it is possible to take properly into account the correlations between α_s and the PDFs central values, though not between α_s and the PDF uncertainties. In this case, the α_s uncertainty is evaluated with PDF sets obtained with the corresponding value of α_s .

For a generic cross section which depends on the PDFs and the strong coupling $\sigma(\text{PDF}, \alpha_s)$, we will have

$$(\delta\sigma)_{\alpha_s}^{\pm} = \sigma\left(\text{PDF}^{(\pm)}, \alpha_s^{(0)} \pm \delta\alpha_s\right) - \sigma\left(\text{PDF}^{(0)}, \alpha_s^{(0)}\right) , \quad (2)$$

where $\text{PDF}^{(\pm)}$ stands schematically for the PDFs obtained when α_s is varied within its 1-sigma range, $\alpha_s^{(0)} \pm \delta_{\alpha_s}$, Eq. 1. Then the overall combined uncertainty will be given by

$$(\delta\sigma)_{\text{PDF}+\alpha_s}^{\pm} = \sqrt{[(\delta\sigma)_{\alpha_s}^{\pm}]^2 + [(\delta\sigma)_{\text{PDF}}^{\pm}]^2}. \quad (3)$$

with $(\delta\sigma)_{\text{PDF}}^{\pm}$ the PDF uncertainty on the observable σ computed from the set with the central value of α_s .

Within the NNPDF approach it is easier to improve the addition in quadrature of the uncertainties and compute the full result using exact error propagation. To compute this full result, we need to recall that the average over Monte Carlo replicas of a general quantity which depends on both α_s and the PDFs, $\mathcal{F}(\text{PDF}, \alpha_s)$, has to be understood schematically as follows

$$\langle \mathcal{F} \rangle_{\text{rep}} = \frac{1}{N_{\text{rep}}} \sum_{j=1}^{N_{\alpha}} \sum_{k_j=1}^{N_{\text{rep}}^{\alpha_s^{(j)}}} \mathcal{F}(\text{PDF}^{(k_j, j)}, \alpha_s^{(j)}), \quad (4)$$

where $\text{PDF}^{(k_j, j)}$ stands for the replica k_j of the PDF fit obtained using $\alpha_s^{(j)}$ as the value of the strong coupling.

The total number of PDF replicas to be used as

$$N_{\text{rep}} = \sum_{j=1}^{N_{\alpha_s}} N_{\text{rep}}^{\alpha_s^{(j)}}, \quad (5)$$

where $N_{\text{rep}}^{\alpha_s^{(j)}}$ is the number of PDF replicas, randomly selected from the fit obtained with the corresponding value of α_s , $\alpha_s^{(j)}$, and N_{α_s} is the number of PDF determinations with different values of α_s which have been performed. The number of replicas for each different value of α_s to be used is thus, for a gaussian distribution,

$$N_{\text{rep}}^{\alpha_s^{(j)}} \propto \exp\left(-\frac{(\alpha_s^{(j)} - \alpha_s^{(0)})^2}{2\delta_{\alpha_s}^2}\right). \quad (6)$$

with $\alpha_s^{(0)}$ and δ_{α_s} given in Eq. 1.

Therefore, within the NNPDF approach the combined $\text{PDF}+\alpha_s$ uncertainty obtained from exact error propagation is given by

$$(\delta\sigma)_{\text{PDF}+\alpha_s}^{\pm} = \sqrt{\langle \sigma^2 \rangle_{\text{rep}} - \langle \sigma \rangle_{\text{rep}}^2}, \quad (7)$$

where the average over replicas (which include PDFs with different α_s) is defined in Eq. 4 (note that here σ denotes a cross-section, and $\delta\sigma$ the uncertainty on it). The comparison between Eq. 7 and Eq. 3 measures the importance of the correlations between PDF and α_s which are not trivially accounted for from the fact that PDF determined from different values of α_s are different.

3 The uncertainty on the PDF uncertainty bands

In order to answer the question of the compatibility of different determinations of PDFs or of physical observables extracted from them it is important that the uncertainties are provided on the quantities which are being compared. Whereas this is standard for central values, it is less frequently done for uncertainties themselves. The systematic way of doing so in a Monte Carlo approach has been reviewed in Ref. [1].

It is important to observe that when addressing the compatibility of two determinations two inequivalent questions can be asked: whether the two determination come from statistically indistinguishable underlying distributions, or whether they come from statistically distinguishable distributions, but are nevertheless compatible.

The determination of the uncertainty on the uncertainty appears to be nontrivial in a Hessian approach, and it has not been addressed so far in the context of Hessian PDF determination to the best of our knowledge. We will thus only discuss it within a Monte Carlo framework. It seems plausible then to assume that uncertainties on uncertainties are of similar size in existing parton fits, so that a difference in uncertainties between two given fits is only significant if it is rather larger than about $\sqrt{2}\sigma[\sigma^2]$, where $\sigma[\sigma^2]$ is the typical uncertainty on a PDF uncertainty.

In a Monte Carlo approach, the uncertainty which should be used when assessing statistical equivalence of two quantities determined from two sets of N_{rep} replicas is the uncertainty of the mean of the replica sample, while the uncertainty to be used when assessing compatibility is the uncertainty of the sample itself, which is larger than the former by a factor N_{rep} [1]. The former vanishes in the limit N_{rep} , while the latter does not: indeed, if the two replica sets come from the same underlying distributions all quantities computed from them should coincide in the infinite-sample size limit, while if they merely come from compatible distributions even for very large sample quantities computed from them should remain different.

Given a set of N_{rep} replicas, the variance of the variance can be determined as [4]

$$\sigma^2[\sigma^2] = \frac{1}{N_{\text{rep}}} \left[m_4[q] - \frac{N_{\text{rep}} - 3}{N_{\text{rep}} - 1} (\bar{\sigma}^2)^2 \right], \quad (8)$$

where σ^2 and m_4 are respectively the variance and fourth moment of the replica sample. Equivalently, we may determine $\sigma^2[\sigma^2]$ by the jackknife method, removing one of the replicas from the sample and determining the N_{rep} variances

$$\sigma_i^2(x) = \frac{1}{N_{\text{rep}} - 2} \sum_{j=1, j \neq i}^{N_{\text{rep}}} (x_j - \mu_i(x))^2; \quad i = 1, \dots, N_{\text{rep}}. \quad (9)$$

The variance of the variance is then given by

$$\sigma^2[\sigma^2] = \sum_{i=1}^{N_{\text{rep}}} \left[(\sigma_i^2)^2 - \bar{\sigma}_i^2 \right], \quad (10)$$

where σ_i^2 is given by Eq. (9) and

$$\bar{\sigma}_i^2 = \frac{1}{N_{\text{rep}}} \sigma_i^2. \quad (11)$$

The quantity $\sigma[\sigma^2]$ estimated using Eq. (8) or equivalently Eq. (10) provides the uncertainty of the sample, and indeed it vanishes in the limit $N_{\text{rep}} \rightarrow \infty$: it should thus be used to assess statistical equivalence. The quantity which should be used to assess consistency is $\sqrt{N_{\text{rep}}}\sigma[\sigma^2]$.

In these document we will compute the uncertainty on the PDF uncertainty in various cases, including in the combined PDF+ α_s uncertainties for all benchmark observables: we will see that the uncertainty on the PDF uncertainty on the benchmark PDF observables is in the range 50 – 70%, thus two PDF sets which yield PDF uncertainties which differ by such an amount are perfectly compatible.

4 Results - LHC 7 TeV

Now we present the results for the LHC 7 TeV scenario. The results are summarized in Table 1. An important result from Table 1 is that PDF and α_s uncertainties can be combined in quadrature for all benchmark processes studied, since this is an excellent approximation to the full error propagation.

The graphical representation of the results of Table 1 can be found in Fig. 1 for W boson production, Fig. 3 for Higgs boson production, and in Fig. 2 for $t\bar{t}$ and Z^0 production, for a mass of the top quark of $m_t = 171.3$ GeV.

In Fig. 4 we show the comparison between the NNPDF2.0 benchmark results with the analogous results obtained from CTEQ6.6 and MSTW08. For these latter fits, we use the both the sets with the default values of α_s and those sets with a common value of $\alpha_s = 0.119$ presented in Refs. [5, 6]. PDF uncertainties for CTEQ6.6 and MSTW08 are assumed to be the same as in the reference analyses.

The benchmark results for the rapidity distributions of vector bosons at LHC 7 TeV are given in Tables 2, 3 and 4, where the combined PDF+ α_s uncertainty obtained with exact error propagation is provided.

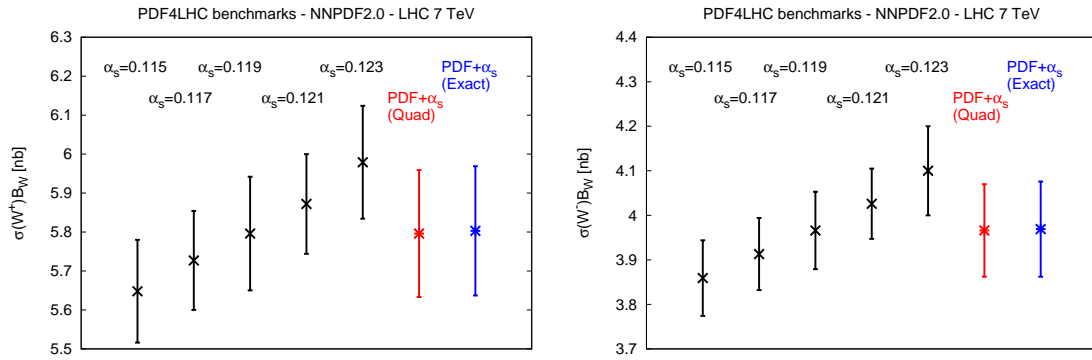


Figure 1: Benchmark results for W^+ and W^- production at the LHC in the 7 TeV scenario.

	$\sigma(W^+)\text{Br}(W^+ \rightarrow l^+\nu_l)$	$\sigma(W^+)\text{Br}(W^+ \rightarrow l^+\nu_l)$
$\alpha_s=0.115$	5.65 ± 0.13 nb	3.86 ± 0.09 nb
$\alpha_s=0.117$	5.73 ± 0.13 nb	3.91 ± 0.08 nb
$\alpha_s=0.119$	5.80 ± 0.15 nb	3.97 ± 0.09 nb
$\alpha_s=0.121$	5.87 ± 0.13 nb	4.03 ± 0.08 nb
$\alpha_s=0.123$	5.98 ± 0.14 nb	4.10 ± 0.10 nb
PDF+ α_s - quad	5.80 ± 0.16 nb	3.97 ± 0.10 nb
PDF+ α_s - exact (1-sigma / 68% CL)	$5.80 \pm 0.17 / \pm 0.14$ nb	$3.97 \pm 0.11 / \pm 0.10$ nb

	$\sigma(Z^0)\text{Br}(Z^+ \rightarrow l^+l^-)$	$\sigma(t\bar{t})$
$\alpha_s=0.115$	886 ± 18 pb	156 ± 5 pb
$\alpha_s=0.117$	898 ± 16 pb	162 ± 5 pb
$\alpha_s=0.119$	909 ± 19 pb	169 ± 6 pb
$\alpha_s=0.121$	921 ± 17 pb	176 ± 6 pb
$\alpha_s=0.123$	937 ± 21 pb	182 ± 7 pb
PDF+ α_s - quad	909 ± 22 pb	169 ± 9 pb
PDF+ α_s - exact (1-sigma / 68% CL)	$910 \pm 22 / \pm 19$ pb	$169 \pm 9 / \pm 9$ pb

	$\sigma(H)(120 \text{ GeV})$	$\sigma(H)(180 \text{ GeV})$	$\sigma(H)(240 \text{ GeV})$
$\alpha_s=0.115$	10.95 ± 0.24 pb	4.23 ± 0.10 pb	2.05 ± 0.05 pb
$\alpha_s=0.117$	11.23 ± 0.18 pb	4.39 ± 0.08 pb	2.10 ± 0.05 pb
$\alpha_s=0.119$	11.60 ± 0.17 pb	4.54 ± 0.09 pb	2.17 ± 0.05 pb
$\alpha_s=0.121$	11.94 ± 0.17 pb	4.68 ± 0.08 pb	2.24 ± 0.05 pb
$\alpha_s=0.123$	12.19 ± 0.19 pb	4.77 ± 0.09 pb	2.29 ± 0.06 pb
PDF+ α_s - quad	11.60 ± 0.39 pb	4.54 ± 0.17 pb	2.17 ± 0.09 pb
PDF+ α_s - exact (1-sigma / 68% CL)	$11.58 \pm 0.36 / 0.38$ pb	$4.53 \pm 0.15 / \pm 0.16$ pb	$2.17 \pm 0.08 / \pm 0.08$ pb

Table 1: Cross sections for W, $t\bar{t}$ and Higgs production at the LHC at $\sqrt{s} = 7$ TeV. All quantities have been computed at NLO using MCFM [7–10] with the PDF4LHC benchmark settings for NNPDF2.0 PDF sets. All uncertainties shown are one-sigma, and for the final PDF+ α_s combined uncertainty we also provide the 68% Confidence Level interval (in parenthesis). We show results for different values of α_s as well as the combined PDF+ α_s results. In the latter case, Eq. 1 is assumed for the α_s central value and uncertainty.

	$d\sigma(W^+)/dy_W \text{Br}(W^+) \text{ [pb]}$	$\delta [d\sigma(W^+)/dy_W \text{Br}(W^+)]_{\text{PDF}+\alpha_s} \text{ [pb]}$
-4.40	2.40	0.32
-4.00	90.43	4.75
-3.60	351.88	19.95
-3.20	588.40	22.75
-2.80	771.20	29.64
-2.40	842.03	30.36
-2.00	861.63	29.27
-1.60	851.36	24.68
-1.20	826.73	39.72
-0.80	830.76	20.41
-0.40	818.77	23.13
0.00	814.72	19.90
0.40	836.49	23.96
0.80	820.44	23.11
1.20	839.94	26.48
1.60	857.90	28.59
2.00	860.17	28.81
2.40	861.25	29.45
2.80	770.78	31.91
3.20	597.95	23.73
3.60	338.32	16.76
4.00	76.01	4.05
4.40	1.58	0.66

Table 2: Benchmark results for the W^+ rapidity distributions at LHC 7 TeV. The uncertainty is the combined PDF+ α_s uncertainty obtained using exact error correlation.

	$d\sigma(W^-)/dy_W \text{Br}(W^-) \text{ [pb]}$	$\delta [d\sigma(W^-)/dy_W \text{Br}(W^-)]_{\text{PDF}+\alpha_s} \text{ [pb]}$
-4.40	0.23	0.25
-4.00	20.57	2.14
-3.60	121.88	7.03
-3.20	278.92	14.34
-2.80	395.40	16.19
-2.40	499.51	19.92
-2.00	569.27	17.61
-1.60	624.32	20.12
-1.20	655.04	14.59
-0.80	687.44	21.08
-0.40	691.53	16.55
0.00	701.12	19.25
0.40	713.34	16.15
0.80	678.39	16.38
1.20	667.26	17.30
1.60	622.98	19.66
2.00	582.53	24.03
2.40	507.60	19.31
2.80	396.65	17.43
3.20	259.80	12.60
3.60	118.70	6.66
4.00	18.47	2.31
4.40	0.31	0.31

Table 3: Benchmark results for the W^- rapidity distributions at LHC 7 TeV. The uncertainty is the combined PDF+ α_s uncertainty obtained using exact error correlation.

	$d\sigma(Z^0)/dy_Z \text{Br}(Z^0)$ [pb]	$\delta [d\sigma(Z^0)/dy_Z \text{Br}(Z)]_{\text{PDF}+\alpha_s}$ [pb]
-4.40	0.01	0.01
-4.00	3.93	0.32
-3.60	30.03	1.53
-3.20	70.36	3.70
-2.80	101.98	4.22
-2.40	124.25	4.29
-2.00	136.34	5.32
-1.60	144.43	3.75
-1.20	147.43	3.93
-0.80	149.92	4.53
-0.40	151.23	3.36
0.00	152.96	4.88
0.40	154.08	3.12
0.80	149.23	4.62
1.20	149.28	4.36
1.60	145.08	3.90
2.00	139.72	5.13
2.40	126.46	4.61
2.80	98.94	4.69
3.20	66.41	3.66
3.60	29.69	2.47
4.00	4.40	0.37
4.40	0.01	0.00

Table 4: Benchmark results for the Z^0 rapidity distributions at LHC 7 TeV. The uncertainty is the combined PDF+ α_s uncertainty obtained using exact error correlation.

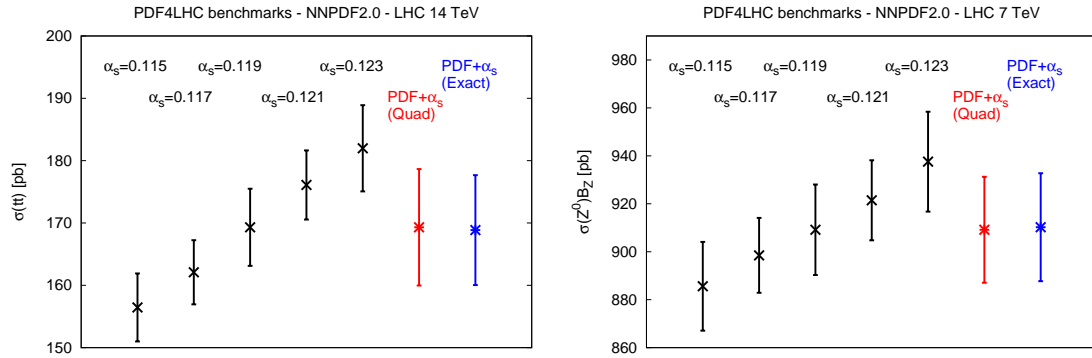


Figure 2: Benchmark results for Z^0 and $t\bar{t}$ production at the LHC in the 7 TeV scenario.

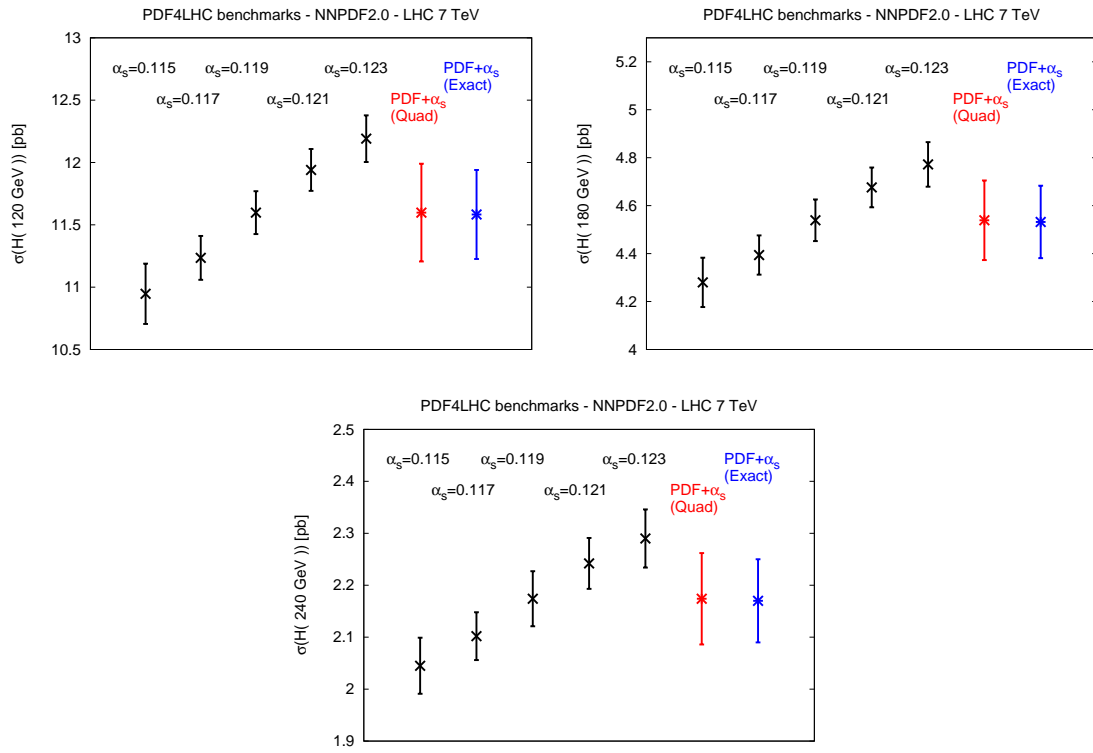


Figure 3: Benchmark results for the Higgs production cross section for $m_H = 120, 180, 240$ GeV in the LHC 7 TeV scenario.

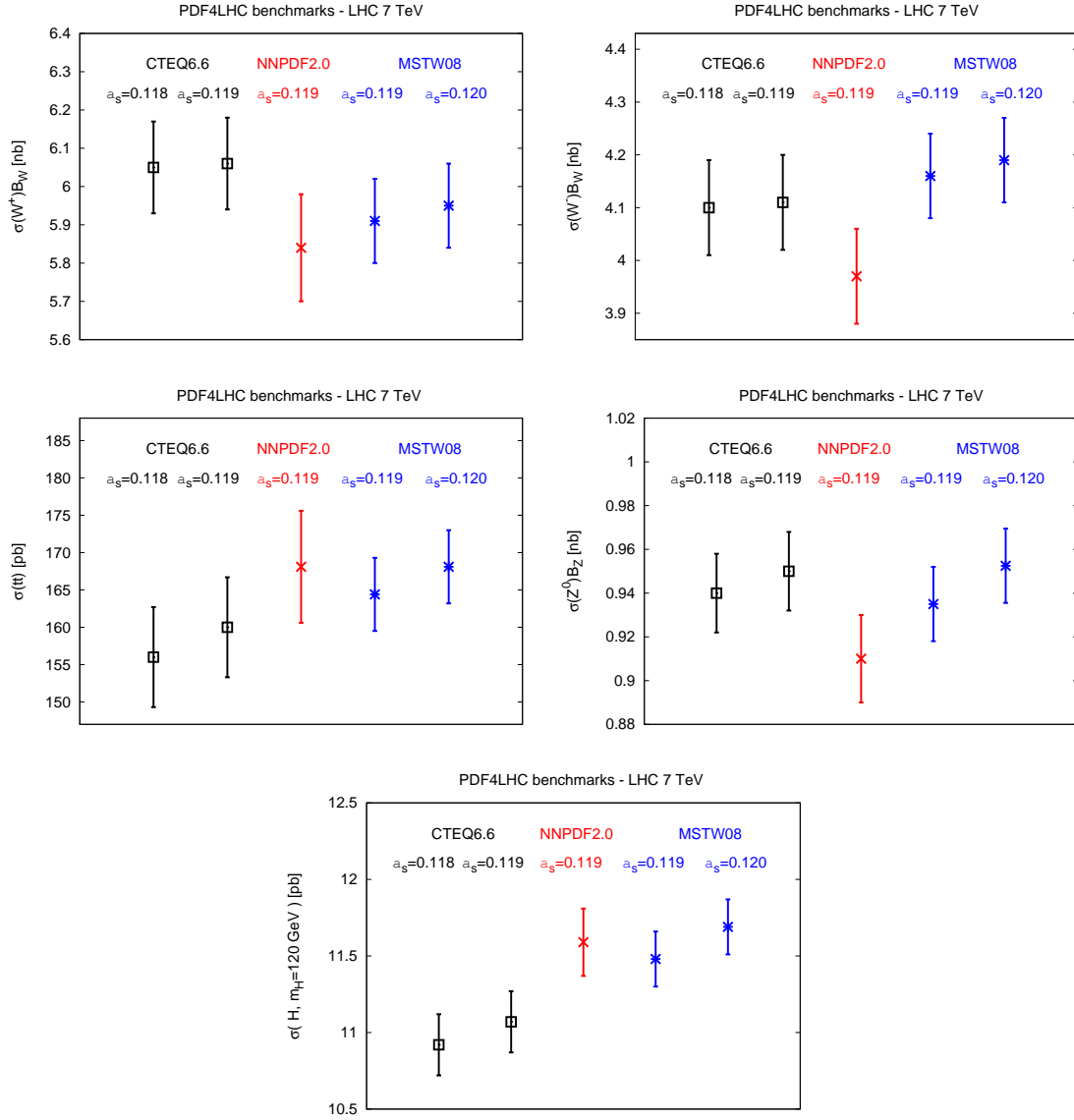


Figure 4: Comparison of benchmark results for NNPDF2.0, MSTW08 and CTEQ6.6 for the LHC 7 TeV scenario.

5 Results - LHC 14 TeV

Now we present the results for the LHC 14 TeV scenario. The results are summarized in Table 5. An important result from Table 5 is that PDF and α_s uncertainties can be combined in quadrature for all benchmark processes studied, since this is an excellent approximation to the full error propagation.

The graphical representation of the results of Table 5 can be found in Fig. 5 for W boson production, Fig. 6 for Higgs boson production, and in Fig. 8 for Z^0 and $t\bar{t}$ production, for a mass of the top quark of $m_t = 171.3$ GeV. For the combined PDF+ α_s uncertainties with exact error propagation, we provide both the 1-sigma and the 68% C.L. uncertainties.

In Fig. 10 we show the comparison between the NNPDF2.0 benchmark results with the analogous results obtained from CTEQ6.6 and MSTW08. For these latter fits, we use the both the sets with the default values of α_s and those sets with a common value of $\alpha_s = 0.119$ presented in Refs. [5, 6]. PDF uncertainties for CTEQ6.6 and MSTW08 are assumed to be the same as in the reference analyses.

The benchmark results for the rapidity distributions of vector bosons at LHC 14 TeV are given in Tables 8, 6 and 7, where the combined PDF+ α_s uncertainty obtained with exact error propagation is provided. These results are represented graphically in Fig. 9.

The uncertainties on the PDF+ α_s combined uncertainties are compared in Table 9 for all benchmark observables. We observe that the uncertainty on PDF uncertainties are in the range 50%-70% depending on the process. Therefore, PDF uncertainties from different PDF sets which differ by such an amount will be compatible. We also see that both the analytical formula and the jackknife method lead to similar results.

It is also clear that processes which are produced by similar parton combinations have a similar relative uncertainty on the PDF uncertainty itself. The PDF uncertainties for different values of α_s and the associated uncertainties on them are compared for various processes in Fig. 7. In this Fig. we assess the statistical equivalence of PDF uncertainties. To assess compatibility, one should multiply error bands by a factor 10.

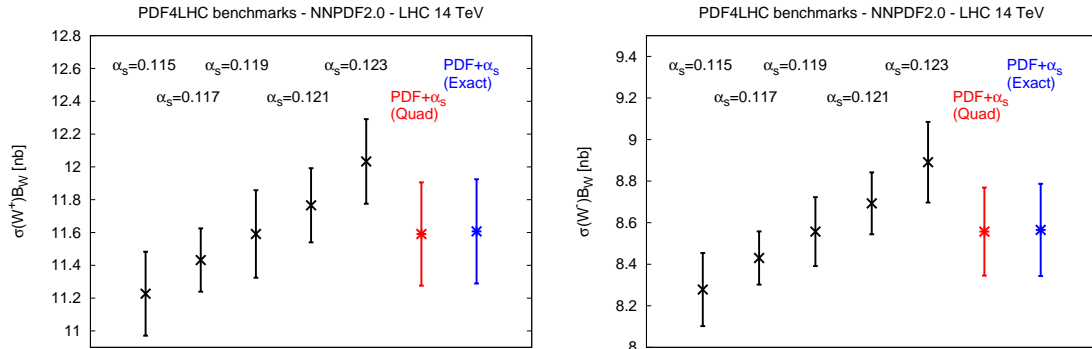


Figure 5: Benchmark results for W^+ and W^- production at the LHC in the 14 TeV scenario.

	$\sigma(W^+)\text{Br}(W^+ \rightarrow l^+\nu_l)$	$\sigma(W^+)\text{Br}(W^+ \rightarrow l^+\nu_l)$
$\alpha_s=0.115$	11.23 ± 0.26 nb	8.28 ± 0.18 nb
$\alpha_s=0.117$	11.43 ± 0.19 nb	8.43 ± 0.13 nb
$\alpha_s=0.119$	11.59 ± 0.27 nb	8.56 ± 0.17 nb
$\alpha_s=0.121$	11.77 ± 0.23 nb	8.69 ± 0.15 nb
$\alpha_s=0.123$	12.03 ± 0.26 nb	8.89 ± 0.19 nb
PDF+ α_s - quad	11.59 ± 0.31 nb	8.56 ± 0.21 nb
PDF+ α_s - exact (1-sigma / 68% CL)	$11.61 \pm 0.32 / \pm 0.28$ nb	$8.56 \pm 0.22 / \pm 0.21$ nb

	$\sigma(Z^0)\text{Br}(Z^+ \rightarrow l^+l^-)$	$\sigma(t\bar{t})$
$\alpha_s=0.115$	1876 ± 37 pb	885 ± 20 pb
$\alpha_s=0.117$	1913 ± 28 pb	910 ± 19 pb
$\alpha_s=0.119$	1939 ± 35 pb	942 ± 21 pb
$\alpha_s=0.121$	1968 ± 30 pb	972 ± 19 pb
$\alpha_s=0.123$	2010 ± 37 pb	995 ± 22 pb
PDF+ α_s - quad	1939 ± 44 pb	942 ± 37 pb
PDF+ α_s - exact (1-sigma / 68% CL)	$1942 \pm 47 / \pm 42$ pb	$940 \pm 34 / \pm 35$ pb

	$\sigma(H)(120\text{ GeV})$	$\sigma(H)(180\text{ GeV})$	$\sigma(H)(240\text{ GeV})$
$\alpha_s=0.115$	35.27 ± 0.66 pb	15.95 ± 0.32 pb	8.63 ± 0.18 pb
$\alpha_s=0.117$	36.17 ± 0.48 pb	16.34 ± 0.23 pb	8.83 ± 0.13 pb
$\alpha_s=0.119$	37.27 ± 0.46 pb	16.83 ± 0.22 pb	9.10 ± 0.13 pb
$\alpha_s=0.121$	38.27 ± 0.43 pb	17.28 ± 0.21 pb	0.35 ± 0.13 pb
$\alpha_s=0.123$	39.15 ± 0.47 pb	17.65 ± 0.23 pb	9.52 ± 0.14 pb
PDF+ α_s - quad	37.23 ± 1.06 pb	16.83 ± 0.51 pb	9.10 ± 0.26 pb
PDF+ α_s - exact (1-sigma / 68% CL)	$37.23 \pm 1.14 / \pm 1.06$ pb	$16.81 \pm 0.47 / \pm 0.50$ pb	$9.09 \pm 0.26 / \pm 0.27$ pb

Table 5: Cross sections for W, Z, $t\bar{t}$ and Higgs production at the LHC at $\sqrt{s} = 14$ TeV. All quantities have been computed at NLO using MCFM [7–10] with the PDF4LHC benchmark settings for NNPDF2.0 PDF sets. All uncertainties shown are one-sigma, and for the final PDF+ α_s combined uncertainty we also provide the 68% Confidence Level interval (in parenthesis). We show results for different values of α_s as well as the combined PDF+ α_s results. In the latter case, Eq. 1 is assumed for the α_s central value and uncertainty.

	$d\sigma(W^+)/dy_W \text{Br}(W^+) \text{ [pb]}$	$\delta [d\sigma(W^+)/dy_W \text{Br}(W)]_{\text{PDF}+\alpha_s} \text{ [pb]}$
-4.80	71.	6.
-4.40	433.	22.
-4.00	866.	43.
-3.60	1144.	50.
-3.20	1361.	51.
-2.80	1417.	66.
-2.40	1412.	49.
-2.00	1451.	48.
-1.60	1403.	38.
-1.20	1390.	52.
-0.80	1414.	43.
-0.40	1403.	44.
0.00	1421.	39.
0.40	1466.	37.
0.80	1420.	49.
1.20	1398.	38.
1.60	1416.	42.
2.00	1447.	51.
2.40	1416.	55.
2.80	1449.	55.
3.20	1388.	55.
3.60	1146.	51.
4.00	816.	36.
4.40	409.	22.
4.80	67.	5.

Table 6: Benchmark results for the W^+ rapidity distributions at LHC 14 TeV. The uncertainty is the combined PDF+ α_s uncertainty obtained using exact error correlation.

	$d\sigma(W^+)/dy_W \text{Br}(W^-) \text{ [pb]}$	$\delta [d\sigma(W^-)/dy_W \text{Br}(W)]_{\text{PDF}+\alpha_s} \text{ [pb]}$
-4.80	15.	3.
-4.40	135.	9.
-4.00	379.	27.
-3.60	603.	31.
-3.20	777.	36.
-2.80	934.	40.
-2.40	1028.	35.
-2.00	1114.	39.
-1.60	1225.	37.
-1.20	1229.	31.
-0.80	1283.	39.
-0.40	1306.	44.
0.00	1325.	41.
0.40	1332.	43.
0.80	1287.	44.
1.20	1254.	37.
1.60	1222.	32.
2.00	1130.	89.
2.40	1034.	90.
2.80	968.	42.
3.20	763.	39.
3.60	577.	30.
4.00	377.	21.
4.40	116.	8.
4.80	14.	3.

Table 7: Benchmark results for the W^- rapidity distributions at LHC 14 TeV. The uncertainty is the combined PDF+ α_s uncertainty obtained using exact error correlation.

	$d\sigma(Z^0)/dy_Z \text{Br}(Z^0)$ [pb]	$\delta [d\sigma(Z^0)/dy_Z \text{Br}(Z)]_{\text{PDF}+\alpha_s}$ [pb]
-4.80	2.84	0.35
-4.40	31.42	1.88
-4.00	95.40	5.23
-3.60	156.03	8.04
-3.20	192.56	8.15
-2.80	223.49	9.18
-2.40	241.43	7.75
-2.00	247.44	6.91
-1.60	269.76	9.30
-1.20	266.98	7.58
-0.80	276.22	11.73
-0.40	277.95	9.90
0.00	282.20	11.43
0.40	286.24	10.70
0.80	275.27	9.57
1.20	270.70	6.88
1.60	266.03	8.18
2.00	251.97	7.53
2.40	244.96	8.82
2.80	230.29	9.33
3.20	187.84	7.07
3.60	151.32	7.37
4.00	93.72	4.72
4.40	29.77	1.60
4.80	2.46	0.36

Table 8: Benchmark results for the Z^0 rapidity distributions at LHC 14 TeV. The uncertainty is the combined PDF+ α_s uncertainty obtained using exact error correlation.

Process	σ	$\sigma(\sigma)$ (%) (I)	$\sigma(\bar{\sigma}) = \sigma(\sigma)/\sqrt{N_{\text{rep}}}$ (%) (I)	$\sigma(\sigma)$ (%) (II)	$\sigma(\bar{\sigma})$ (%) (II)
W^+	0.31 nb	78	7.8	72	7.2
W^-	0.22 nb	77	7.7	70	7.0
Z^0	47 pb	78	7.8	71	7.1
h(120)	1.06 pb	61	6.1	50	5.0
h(180)	0.47 pb	61	6.1	50	5.0
h(240)	0.26 pb	62	6.2	51	5.1
$t\bar{t}$	34.4 pb	65	6.5	56	5.6

Table 9: The uncertainty on the combined PDF+ α_s uncertainties in all the benchmark observables at LHC 14 TeV, computed both with the analytical expression (I), Eq. 8, and with the jackknife method (II), Eq. 10.

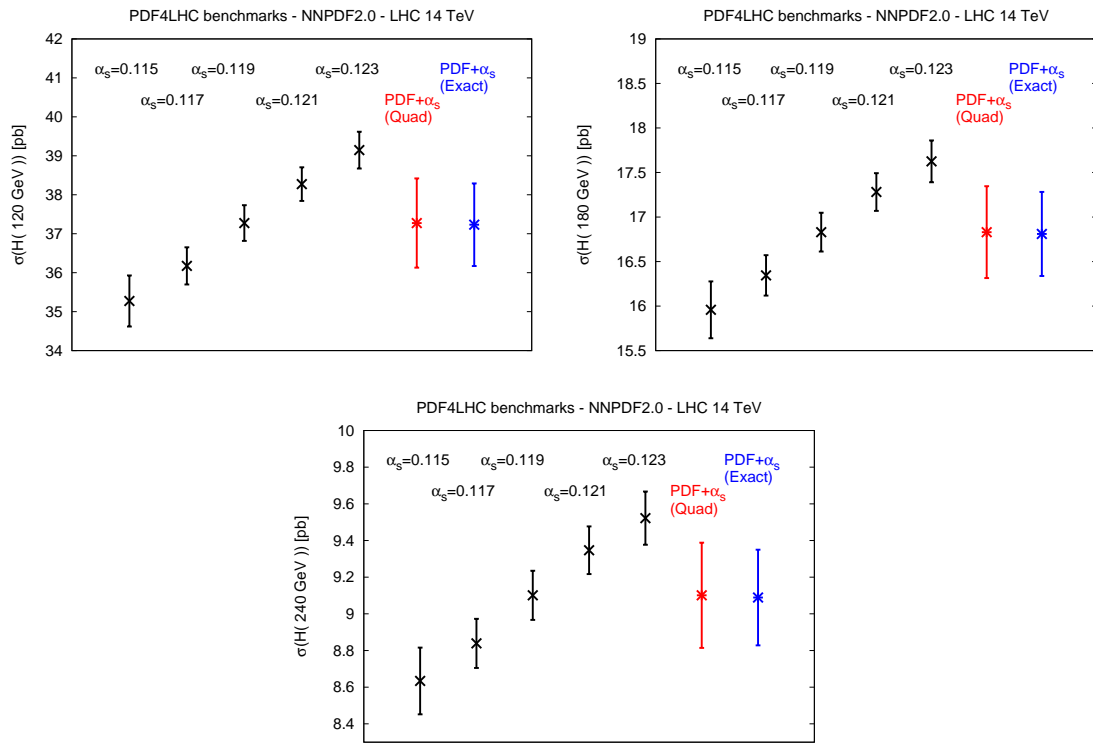


Figure 6: Benchmark results for the Higgs production cross section for $m_H = 120, 180, 240$ GeV.

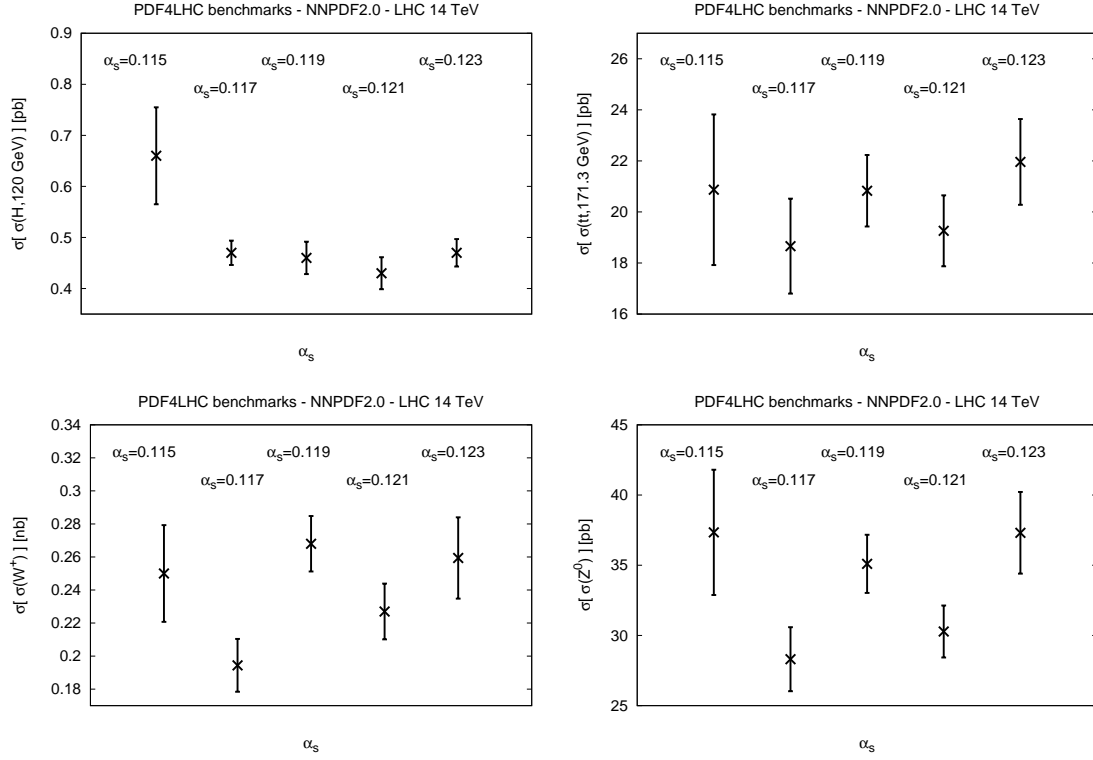


Figure 7: Comparison of the PDF uncertainties in: Higgs boson production cross sections for $m_H = 120$ GeV, $t\bar{t}$ production and W^+ and Z^0 production at the LHC 14 TeV, for different values of α_s . The error bars correspond to the uncertainty in the PDF uncertainties itself, as computed with the jackknife method, Eq. 10. Note that in this plot we are assessing the statistical equivalence of fits obtained with different α_s .

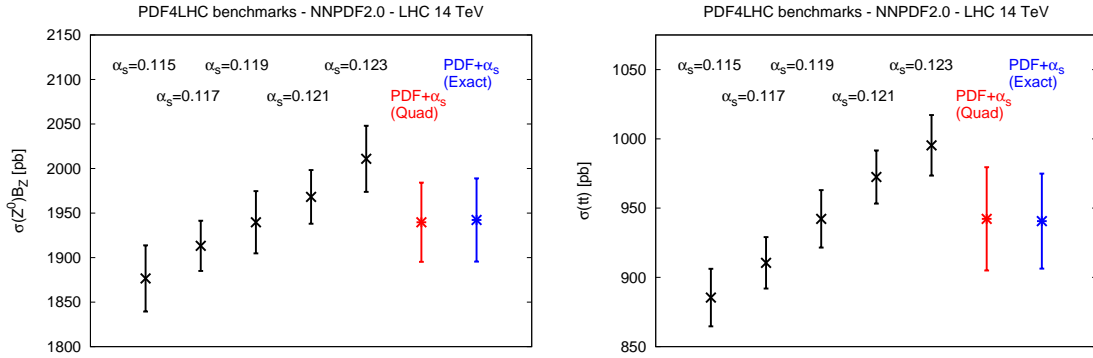


Figure 8: Benchmark results for Z^0 and $t\bar{t}$ production at the LHC in the 14 TeV scenario.

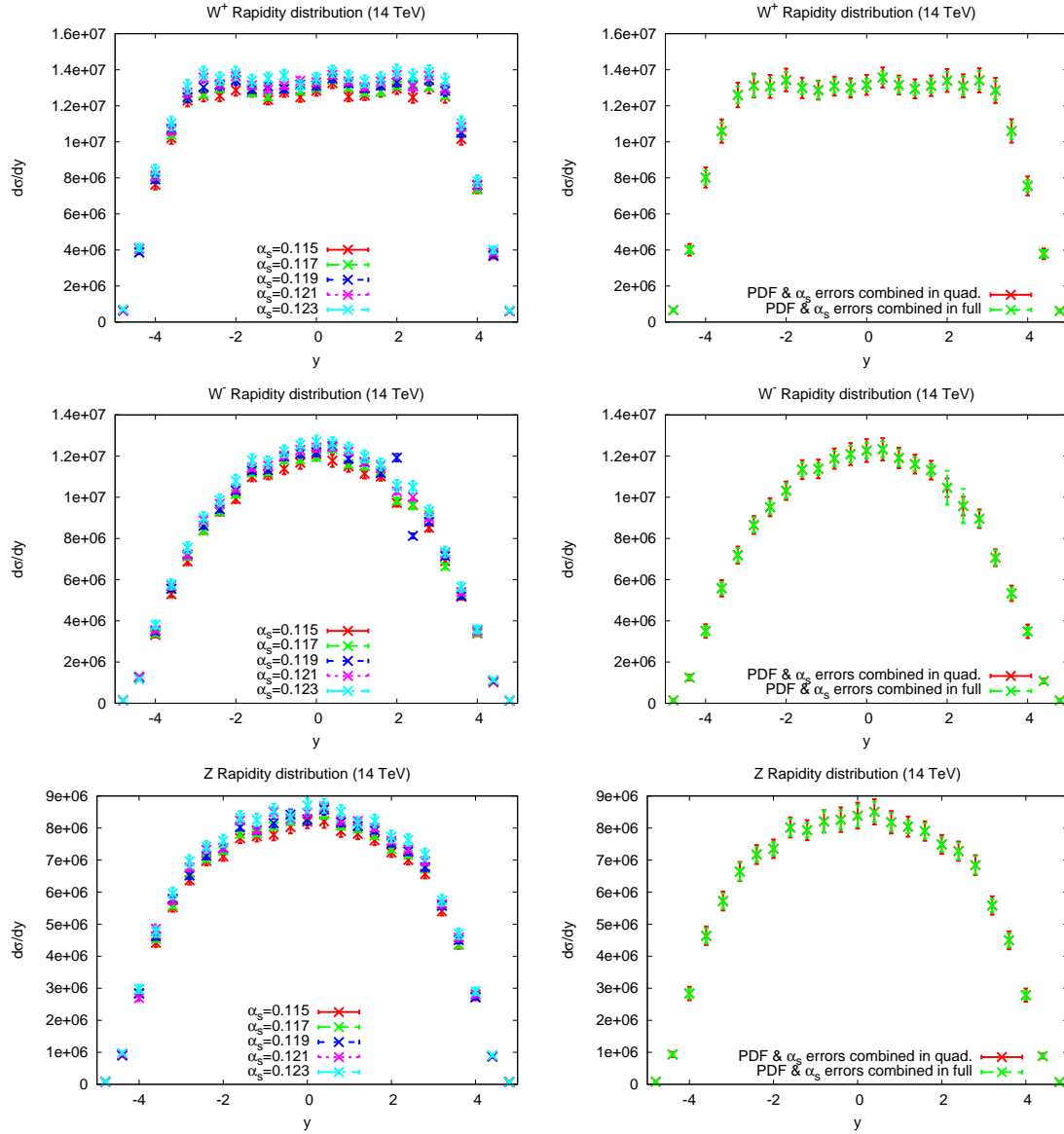


Figure 9: Benchmark results for the rapidity distributions in vector boson production in the LHC 14 TeV scenario. From top to bottom: W^+ , W^- and Z rapidity distributions. The left plots show the results for the PDF sets with different α_s while the right plots show the results with the combination of PDF and α_s uncertainties, both with exact error propagation or and adding PDF and α_s uncertainties in quadrature.

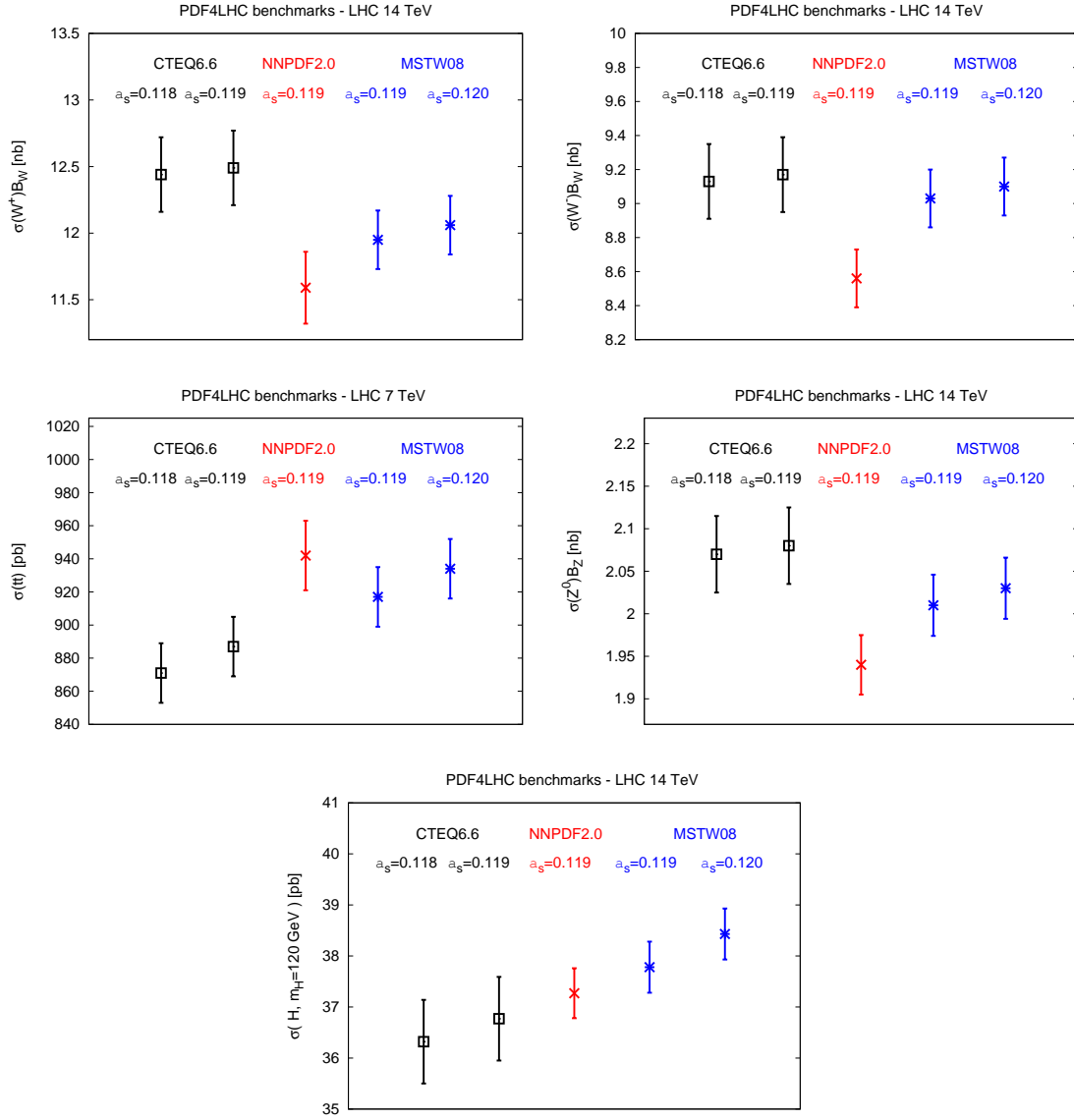


Figure 10: Comparison of benchmark results for NNPDF2.0, MSTW08 and CTEQ6.6 for the LHC 14 TeV scenario.

6 Results - Tevatron

The only PDF4LHC benchmark process which has been proposed for the Tevatron is inclusive jet production. In Fig. 11 we show the PDF and combined PDF+ α_s uncertainties for inclusive jet production at the Tevatron, in particular the first rapidity bin of the CDF Run II kt measurement as computed with FastNLO [11].

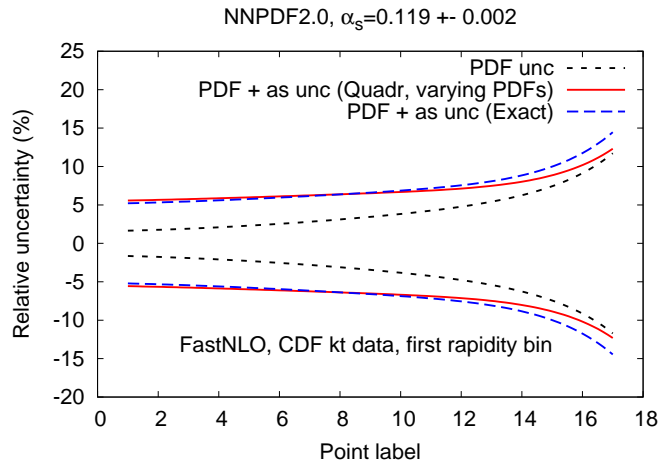


Figure 11: Benchmark results for inclusive jet production at the Tevatron.

References

- [1] R.D. Ball et al., (2010), 1002.4407.
- [2] T. Binoth et al., (2010), 1003.1241.
- [3] F. Demartin et al., (2010), 1004.0962.
- [4] Particle Data Group, C. Amsler et al., Phys. Lett. B667 (2008) 1.
- [5] A.D. Martin et al., Eur. Phys. J. C64 (2009) 653, 0905.3531.
- [6] H.L. Lai et al., (2010), 1004.4624.
- [7] J.M. Campbell and R.K. Ellis, Phys. Rev. D62 (2000) 114012, hep-ph/0006304.
- [8] J. Campbell and R.K. Ellis, Phys. Rev. D65 (2002) 113007, hep-ph/0202176.
- [9] J. Campbell, R.K. Ellis and F. Tramontano, Phys. Rev. D70 (2004) 094012, hep-ph/0408158.
- [10] MCFM, <http://mcfm.fnal.gov>.
- [11] T. Kluge, K. Rabbertz and M. Wobisch, (2006), hep-ph/0609285.